

© Copyright 1990 American Meteorological Society (AMS). Permission to use figures, tables, and brief excerpts from this work in scientific and educational works is hereby granted provided that the source is acknowledged. Any use of material in this work that is determined to be “fair use” under Section 107 of the U.S. Copyright Act or that satisfies the conditions specified in Section 108 of the U.S. Copyright Act (17 USC §108, as revised by P.L. 94-553) does not require the AMS’s permission. Republication, systematic reproduction, posting in electronic form on servers, or other uses of this material, except as exempted by the above statement, requires written permission or a license from the AMS. Additional details are provided in the AMS CopyrightPolicy, available on the AMS Web site located at (<http://www.ametsoc.org/AMS>) or from the AMS at 617-227-2425 or [copyright@ametsoc.org](mailto:copyright@ametsoc.org).

Permission to place a copy of this work on this server has been provided by the AMS. The AMS does not guarantee that the copy provided here is an accurate copy of the published work.

Margita C. Liepins, Marilyn M. Wolfson, David A. Clark, and Barbara E. Forman  
M.I.T. Lincoln Laboratory  
Lexington, Massachusetts 02173

## 1. INTRODUCTION

The Federal Aviation Administration (FAA) currently uses the anemometer-based Low Level Wind Shear Alert System (LLWAS) as the primary method of wind shear detection at major U.S. airports. With the upcoming deployment of the Terminal Doppler Weather Radar (TDWR) system (Turnbull et al. 1989), potential methods for integrating the two systems are being investigated. By integrating, the advantages of both sensor systems can be utilized. Advantages of the LLWAS ground sensor network include true wind direction measurements, a high measurement frequency, a lack of sensitivity to clear air reflectivity, and few false alarms from radar point targets such as planes, birds, etc. Advantages of the radar include complete scan coverage of the region of concern, the ability to predict events, fewer terrain problems such as sheltering which can reduce the wind speed readings, and almost no false alarms due to non-hazardous wind shear such as thermals.

The objectives of this study are to gain a clearer understanding of the basic relationship between the wind information provided by these two very different sensing systems, and to determine the impact this relationship may have on integration of the two operational systems. A proposed mathematical technique for "correcting" LLWAS winds where needed to better match radar winds is evaluated for cases of microburst (divergent) and gust front (convergent) wind shear.

## 2. THE STUDY

In this study we use a large base of Doppler radar and anemometer data to determine a numerical relationship between the respective wind measurements. This relationship is influenced by:

1. Actual wind differences within the sampling spaces used by the two sensors. These include differences due to sampling height, and effects of local anemometer obstructions (both sheltering and channeling of wind).
2. Effects resulting from the different sensing methodology, or from physical characteristics of the actual sensors.

A number of studies have been conducted to measure the change of wind speed with height by mounting wind sensors on meteorological towers or on existing television tow-

ers. In general, a power law has been found to best describe the wind profile in the frictional boundary layer (e.g. Joffre 1984). This profile is generally dependent on the temperature lapse rate and ground roughness (Haltiner and Martin 1957). For this study, we chose to use the power law profile to represent the winds measured by the anemometer and radar since it provides for a nonlinear solution that accounts for the inherent difference in sampling height. The power law profile is stated:

$$U / U_1 = (Z / Z_1)^p \quad (2.1)$$

where  $U$  and  $U_1$  represent the wind speeds at heights  $Z$  and  $Z_1$  respectively and  $0 \leq p \leq 1$ . The exponent  $p$  is empirically derived by comparing a large number of radar and anemometer wind values measured during a variety of wind shear events. In our case  $p$  is dependent not only on the lapse rate and ground roughness, but on the inherent differences in the two sensors.

## 3. METHODOLOGY

### 3.1 Data

Doppler weather radar and surface anemometer data were collected during 1988 in Denver, CO as part of the FAA TDWR measurement program and operational demonstration. Doppler wind measurements were collected with an S-Band radar (FL-2) developed and operated by Lincoln Laboratory (Evans and Turnbull 1989), while surface ane-

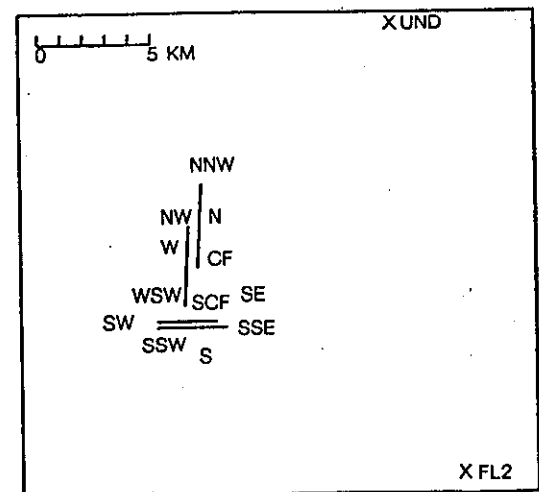


Figure 1. The 1988 LLWAS network at Stapleton International Airport in Denver, CO. The runways are denoted by the two pairs of straight lines. UND and FL-2 radar locations are indicated (X) in the upper and lower right corners respectively.

\*The work described here was sponsored by the Federal Aviation Administration. The United States Government assumes no liability for its content or use thereof.

mometer wind measurements were collected from twelve LLWAS sensors situated in the vicinity of Denver's Stapleton International Airport. Dual-Doppler data were created using the University of N. Dakota C-Band radar (UND) and FL-2 (Figure 1).

Twelve cases were chosen to include a variety of meteorological events and wide range of radar reflectivity values. Cases included gust fronts, microbursts, areas of divergence, and areas of widespread strong winds that occurred from mid-May to mid-August, and covered time periods of approximately one-half to two hours each (Table 1).

### 3.2 Comparing Radar and Anemometer Winds

Doppler wind measurements were taken from the lowest elevation scan (either 0.3° or 0.4°) which typically updated at a rate of approximately once per minute. A signal-to-noise ratio (SNR) threshold of 6 dB was applied to reduce noisiness in the data. Doppler (radial) velocity measurements were then read from the radar gate closest in range and azimuth to each LLWAS station location, and from the eight surrounding gates. The radar gate size was 120 m in the radial direction and varied from approximately 200 m to 300 m azimuthally depending upon radar range. The median Doppler velocity value from the nine gates was then used for comparison with the corresponding radial component of LLWAS wind, provided at least four of the gates were not flagged as "bad data", or empty due to SNR thresholding. This filtering reduced the effect of gates which were contaminated with ground clutter or point targets.

LLWAS wind measurements are made every 6-7 seconds, so insignificant as well as significant wind fluctuations

were recorded. Cornman et al. (1989) defined a "significant fluctuation" model as an objective basis for identifying wind shear events. The most recent automated LLWAS wind shear detection algorithm (Cornman and Wilson 1989; UCAR 1990) attempts to eliminate insignificant fluctuations by applying a running weighted mean filter covering approximately 60-90 seconds in time. A similar approach was taken here, except the values included in the 1 minute average were evenly weighted.

The height of the center of the radar beam above the surface anemometer ranged from approximately 150 m to 250 m. The heights above ground level of the 12 LLWAS anemometers are shown in Figure 2. In 1988, they ranged

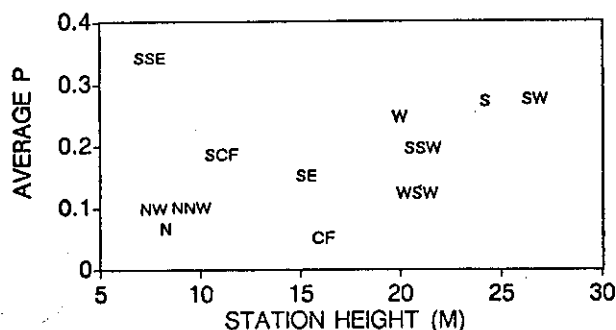


Figure 2. Plot of the average value of the exponent  $p$  versus station height.

from 7.6 m to 26.8 m. (Some anemometer heights have since been raised to reduce sheltering.)

Table 1. Chart showing the date, description, reflectivity, Doppler wind speed range, and number of data points for each case. The number of data points refers to the average number of valid radar data points per station with SNR > 6 dB, suitable for comparison with LLWAS data. [\* denotes case where 46% of the radar data containing the wind shear event were invalid after SNR thresholding and much of the valid data was just above threshold. Data from this case were not used in the study.]

DATE (1988)	DESCRIPTION	DBZ	WINDS m/s	# DATA POINTS
10 MAY 19:15-21:00	widespread rain, solid wind field	25 - 30	-10 -> +2	48
18 MAY 21:00-22:00	multi-cell storm with some divergence, turns into a line storm	up to 60	-12 -> +7	34
09 JUN 20:50-22:15	weak widespread cells	20 - 30	+2 -> +7	54
09 JUN 23:30-23:59	widespread winds, convergence line	up to 35	-12 -> +12	17
25 JUN 20:00-20:40	line storm moving westward, gf at N end of the network	up to 50	-15 -> +5	26
07 JUL 00:00-01:00	10 km storm cell	up to 55	0 -> +10	42
11 JUL 22:00-23:00	region of widespread rain, strong microbursts in the SE corner of the network	up to 40	-12 -> +7	41
16 JUL 22:00-23:59	10 km cellular storm moves N to S divergent line at 22:50, microburst 23:08-23:35	20 - 55	-15 -> 0 -12 -> +12	84
17 JUL 21:35-22:00	compact 10 km line cell	10 - 25	-15 -> -10	51
29 JUL 22:30-23:59	isolated 5 km cells over the network, turns into a line storm by 23:50	up to 55	+5 -> +12.5	50
09 AUG 18:30-20:00	microburst located in the N end of the network	up to 15	+10 -> -15	0*
21 AUG 88 21:15-22:00	cellular storm at the S end of the network becomes widespread winds	40 - 45 up to 30	0 -> +5 -5 -> -8	30

### 3.3 Derivation of Power Law Exponent

The power law profile provides a model of the atmospheric boundary layer by which the relationship between radar and surface wind measurements may be assessed. Referring to Eq. (2.1), values for  $p$  were calculated for each LLWAS station by using the Doppler velocity as  $U$ , the radial component of the LLWAS wind as  $U_1$ , the height of the radar gate above the LLWAS station as  $Z$ , and the height of the LLWAS station above the ground as  $Z_1$ . Data from the twelve cases provided 5773 values of  $p$  for the 12 stations.

From this data set, the probability density versus the value of  $p$  was plotted. The plots yielded an approximately normal distribution for each station (see Figure 4), as measured by the  $\chi^2$  goodness-of-fit test. The mean value of  $p$  and the standard deviation were calculated for each station. These values are shown in Table 2, and also indicated in Figure 4.

Table 2. Statistical data from derivation of power law relationship for twelve LLWAS stations.

station	$\bar{p}$	$\sigma$	$\bar{p} - 1/2\sigma$	multiplier $(z/z_1)^p$ implied by:	
				$\bar{p}$	$\bar{p} - \sigma/2$
CF	0.050	0.139	-0.020	1.10	0.95
SCF	0.186	0.142	0.109	1.51	1.37
W	0.246	0.126	0.183	1.49	1.53
NW	0.100	0.109	0.039	1.29	1.14
NNW	0.101	0.175	0.012	1.27	1.04
N	0.069	0.120	0.009	1.19	1.03
SE	0.152	0.169	0.067	1.37	1.19
SSE	0.340	0.235	0.223	2.40	2.07
S	0.270	0.264	0.138	1.46	1.34
SSW	0.196	0.144	0.124	1.36	1.32
SW	0.277	0.263	0.146	1.44	1.34
WSW	0.126	0.192	0.001	1.22	1.00

### 3.4 Discussion of results

We found a large variation for the twelve stations, and a significant range of variances as well. Wind speeds measured at stations CF and N are most representative of the radar wind speed, with near-zero  $\bar{p}$  values implying an excellent anemometer exposure. Station SSE shows the

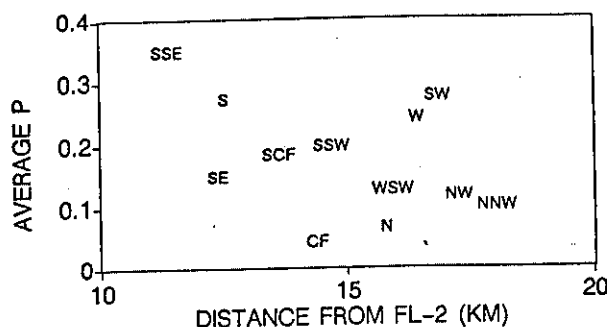


Figure 3. Plot of the average value of the exponent  $p$  versus station distance from the FL-2 radar.

most difference, with  $\bar{p} = 0.4$ . Notice also how low the variance of the  $p$  distribution is for this station; the wind speeds measured at SSE are always too slow. This may indicate the need to raise the anemometer or replace the bearings. The large  $\bar{p}$  values at stations S, SW, and W also imply a large difference between the LLWAS and radar wind speeds. There appears to be little correlation between the variability of  $\bar{p}$  with either the height of the LLWAS station (Figure 2) or its distance from the radar (Figure 3). The measured differences can be fairly confidently attributed to anemometer exposure and sensor maintenance at the different LLWAS sites.

## 4. APPLICATION

The representation of the difference in measured wind speed between the radar and LLWAS with a power law profile provides a useful method for "adjusting" the LLWAS speed to some radar height equivalent. For a constant radar height, e.g. the average height of the lowest tilt over the LLWAS network, the adjustment to the LLWAS speed becomes linear for an individual station, represented by  $(Z/Z_1)^p$ . Statistically, this would yield an overestimate with respect to the radar equivalent wind speed 50% of the time.

For practical application, it is prudent to take a more conservative approach and reduce the power law exponent by some amount dependent upon the variance of  $p$  for a particular station. For instance, reducing  $\bar{p}$  by one standard deviation would reduce the probability of overestimation to 16%. This, however, would also reduce the adjustment to a negligible amount. Since analysis of the error variance of the sample data indicated that a large portion of the overestimated winds were associated with low wind speed values, it would seem reasonable to take an intermediate approach and reduce the exponent by one-half standard deviation. This appears to provide a reasonable wind speed adjustment with a sufficiently low percentage of overcorrection (30%).

Table 2 also includes the multiplication factors for adjustment of LLWAS wind speeds to a radar equivalent, using both the  $\bar{p}$  and  $\bar{p} - \sigma/2$  as the exponent in the power law relationship, and a typical radar scan height of 200 m.

### 4.1 Microburst Case Study

In order to observe the potential impact of the LLWAS wind adjustment, we applied it to data from a strong microburst event which affected flight operations at Stapleton Airport on 11 July 1988 (Schlickenmaier 1989). The microburst developed as a series of pulses along a line to the east and south of the east-west runways from 2206-2221 UTC. Figure 5 shows LLWAS wind plots at two instances during the microburst period. Figure 5 (a) (2209:22 UTC) shows the location of two main pulses (labeled A and B) along the microburst line. The locations of these pulses were determined through analysis of single- and dual-Doppler radar data, and supplemental surface anemometer data. By 2211:21 UTC [Figure 5 (b)], a third pulse (C) is identified near station SSE. Pulse B ultimately provided the strongest shear, as radar data indicated more than 80 knots of headwind loss to the east of the east-west runways. The shear from this pulse, however, was beyond the range of the LLWAS network and not fully sensed by the anemometer system.

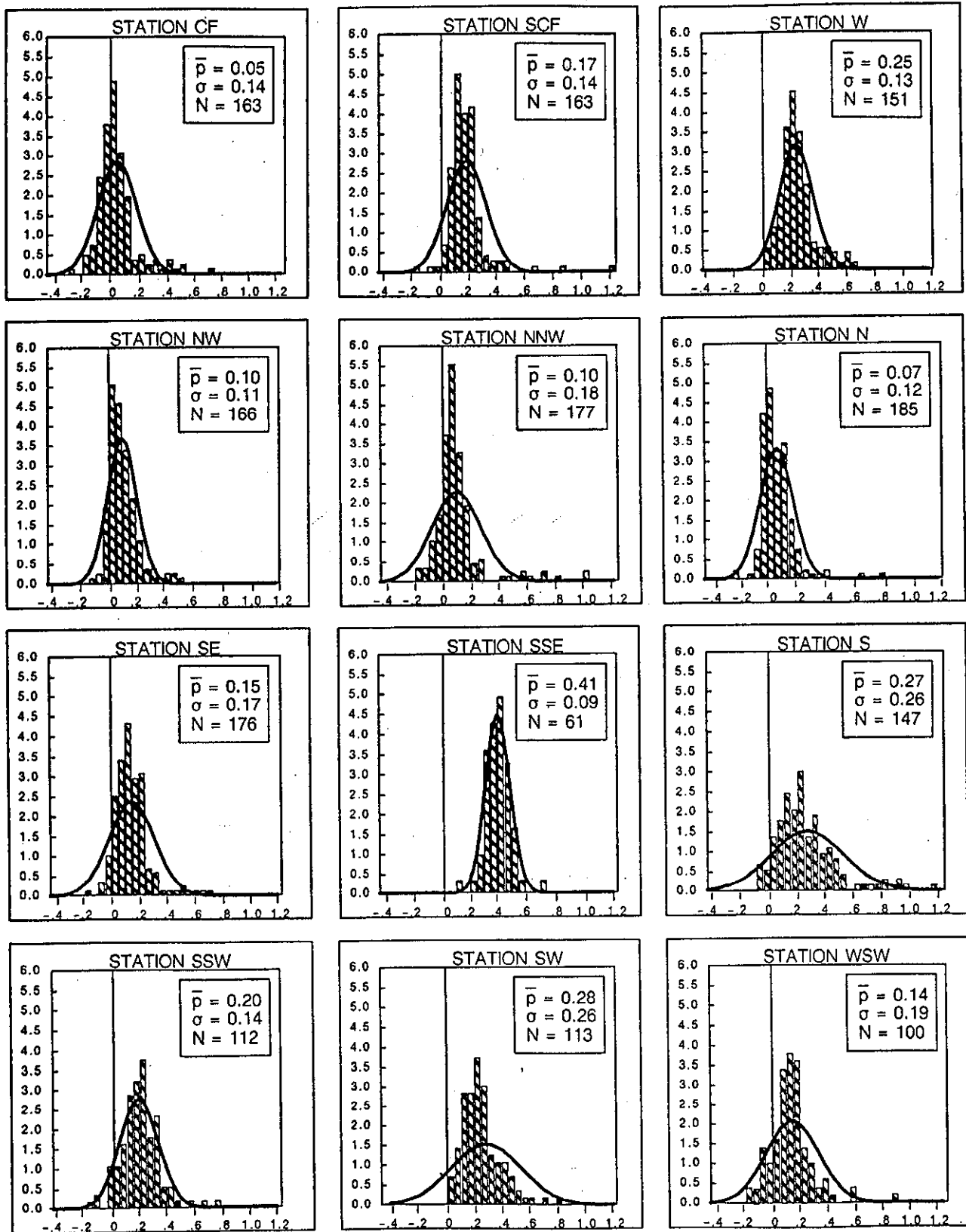


Figure 4. Histogram plots of the probability density of  $p$  for each station where  $\bar{p}$  is the value of the power law profile exponent,  $\sigma$  is the standard deviation, and  $N$  is the total number of data points used to determine the distribution.

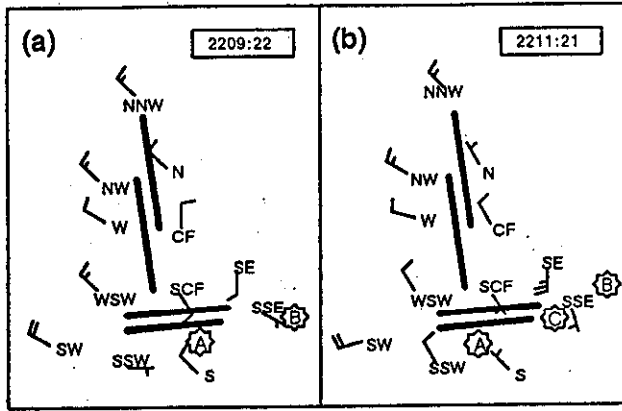


Figure 5. LLWAS winds for 11 July 1988 at a) 2209:22 UTC and b) 2211:21 UTC. One full barb represents 10 m/s. Runways are denoted by bold straight lines. Positions of main microburst pulses are lettered A, B, and C.

The LLWAS winds (adjusted and unadjusted) were compared with wind vectors from dual-Doppler radar data, with particular attention to those stations affected by the microburst, namely SE, SSE, SCF, S, and SSW. The LLWAS wind speeds were adjusted to a height of 200m above ground

level (the approximate average height of the low-elevation tilts over the network), conservatively applying the power law by reducing the empirical value of  $\bar{p}$  by  $\sigma/2$ . The adjustment of the LLWAS wind speed made it more consistent with the dual-Doppler wind, prior to the microburst. However, once the microburst winds began to affect a station, the LLWAS wind speed was greater than that from dual-Doppler data, and the adjustment of the LLWAS wind actually increased the difference in wind speed as measured by the two systems.

Two examples of this overcorrecting are shown in Figure 6. At station SSE, the adjustment to the LLWAS wind speed makes it more consistent with the dual-Doppler speed up until 2208 UTC, at which time there is a spike in the wind speed resulting from the nearby microburst. For the next few minutes, the LLWAS speed is either equal to or greater than that measured from dual-Doppler data, and the adjustment of the LLWAS wind results in a greater difference from the dual-Doppler wind. A similar affect is seen at Station SE [Figure 6 (b)], as the third pulse in the microburst caused a wind speed spike shortly after 2210 UTC, at which time the LLWAS wind speeds generally exceed the radar speeds. A possible explanation for this overcorrecting is discussed in section 4.3.

#### 4.2 Gust Front Case Study

On 17 July 1988 a strong gust front traversed the LLWAS network shortly after 2130 UTC with the strongest component of wind oriented radially with respect to the FL-2 radar. Unlike the previous microburst case in which the strong winds developed impulsively from a downdraft directly over the LLWAS network, the strong winds were propagated over the network from the northwest. Figure 7 shows both the unadjusted and adjusted radial component wind speed traces for two LLWAS stations as compared to the radar-measured wind.

For Station SSE, statistical analysis yielded a significant adjustment for the LLWAS wind speed (Station SSE has the highest adjustment factor). It can be seen in [Figure 7 (a)] that this adjustment to the LLWAS wind speed is successful in bringing the LLWAS winds closer to the radar winds. In the case of station SCF [Figure 7 (b)], where statistical analysis yielded a much smaller adjustment to the LLWAS winds, the results are very similar to Station SSE in that the LLWAS wind estimate is greatly improved. LLWAS winds are not overcorrected in either case.

#### 4.3 Discussion

The overcorrection by the empirical power law relationship during the microburst (divergent) wind shear event may be explainable by the deviation from the typical vertical wind profile within the lower boundary layer during a microburst [Figure 8 (a)]. As the microburst reaches the ground, its downward momentum locally perturbs the vertical wind profile, and the horizontally divergent wind results in a very thin layer of very high wind speeds near the ground. In contrast, the boundary layer wind profile in a gust front [Figure 8 (b)] conforms better to that modelled with an average power law profile. Also, the radar measurement of wind over a pulse volume in this case more nearly equals

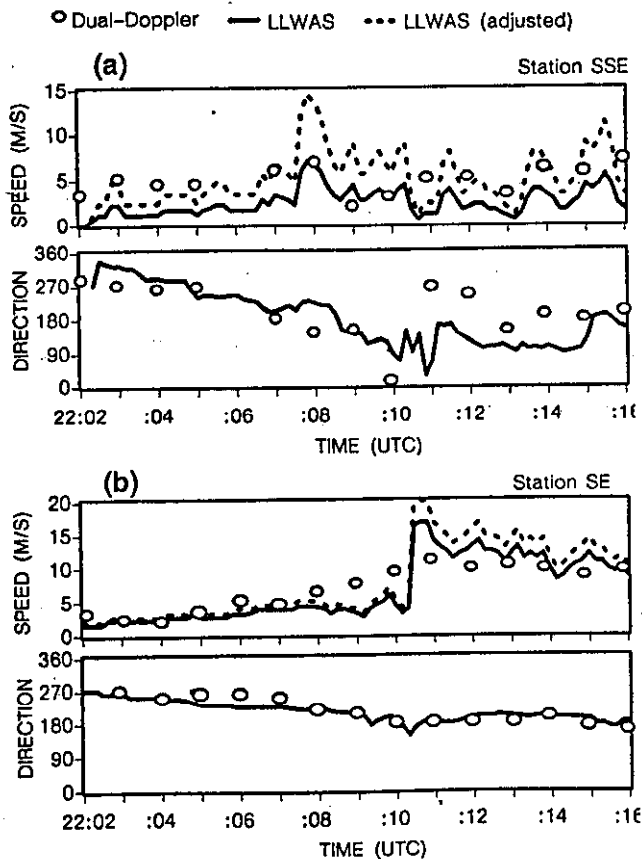


Figure 6. Time series plots of wind speed and direction for LLWAS (solid line), adjusted LLWAS (dashed line), and dual-Doppler synthesized winds (circles) for LLWAS stations a) SSE and b) SE during a microburst event.

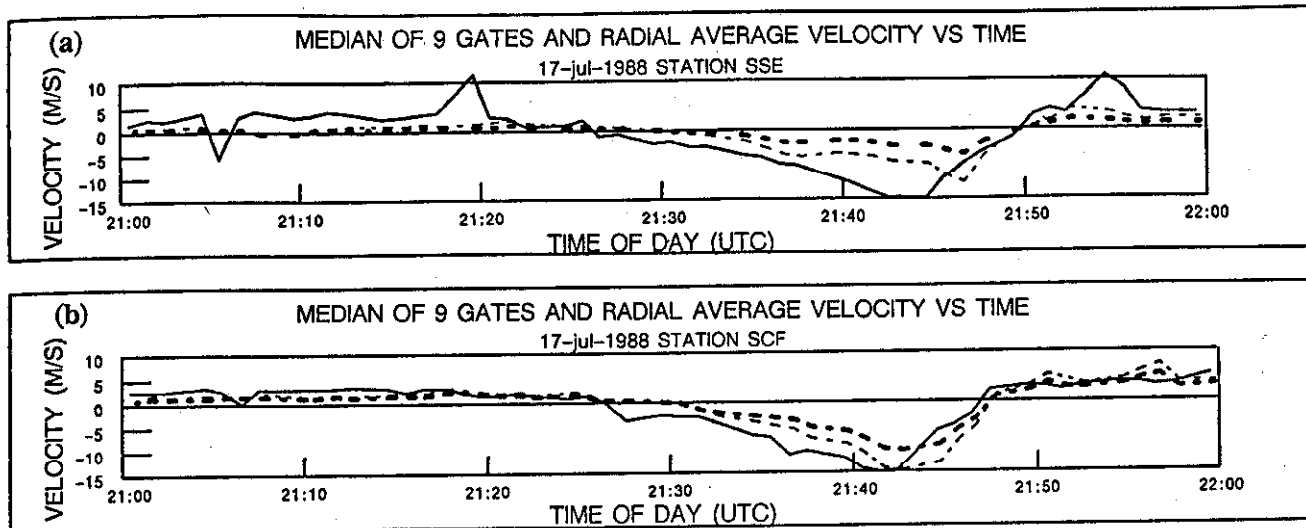


Figure 7. Plot of radial component of wind speeds with respect to FL-2 as measured by radar (solid line), LLWAS (bold dashed line), and adjusted LLWAS (dashed line) at location of LLWAS stations a) SSE and b) SCF.

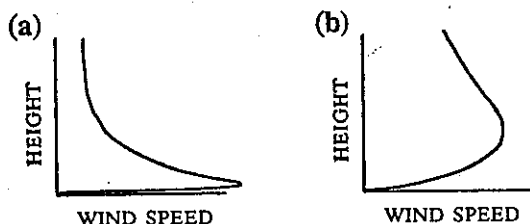


Figure 8. Schematic illustration of wind speed profile for surface conditions a) with strong divergent wind shear, and b) strong persistent straight line winds.

a point measurement, because the wind speed variations with height are smaller.

## 5. CONCLUSIONS

It has been found that wind speed measurements by surface anemometers and by Doppler radar were, in general, quite comparable over the Denver 1988 LLWAS network for a set of 11 days with appreciable weather. We used the exponent  $p$  from the power law shown in Eq. (2.1) as an indicator of the correlation between surface and radar wind speeds. In Figure 4 it can be seen that the highest probability density of  $p$  occurs fairly close to zero for most of the stations. Such  $p$  values imply the need for little or no correction of surface wind speeds. A few of the stations (i.e. SSE, S, W, and SW) show higher  $p$  values. These higher values are most likely the result of poor anemometer siting or a mechanical problem with the sensor. The best solution would be to resite or raise the anemometer, but this is not always possible. The possibility of providing the necessary correction numerically using the power law profile was evaluated.

A closer look at the data reveals that during microburst conditions, where a strong downdraft results in a horizontal spreading of air close to the surface, the two sensors

yield equivalent speeds. During such events the application of a wind speed correction factor is not necessary and could result in the overestimation of ground wind speeds. In the case of a gust front, however, where winds are generally parallel to the surface and penetrate the surface boundary layer to a lesser extent, the comparison between the two sensors is not as good. It has been shown that in these cases the application of a correcting factor can make LLWAS winds more comparable to Doppler radar winds.

## 6. REFERENCES

- Cornman, L.B., P.C. Kucera, M.R. Hjelmfelt, and K.L. Elmore, 1989: Short time-scale fluctuations in microburst outflows as observed by Doppler radar and anemometers. Preprints, *24th Conference on Radar Meteorology*, Tallahassee, FL, Amer. Meteor. Soc., 150-153.
- Cornman, L.B., and F.W. Wilson, Jr., 1989: Microburst Detection from Mesonet Data. *3rd International Conference on the Aviation Weather System*, Anaheim, CA, 35-40.
- Evans, J.E., and D.H. Turnbull, 1989: Development of an automated windshear detection system using Doppler weather radar. *Proc. IEEE*, 77, 1661-1673.
- Haltiner, G.J., and F.L. Martin, 1957: *Dynamical and Physical Meteorology*. McGraw-Hill, New York, 228-233.
- Joffre, S.M., 1984: Power laws and the empirical representation of velocity and directional shear. *J. Appl. Meteor.*, 23, 1196-1203.
- Schlickenmaier, H.W., 1989: Windshear Case Study: Denver, Colorado, July 11, 1988. *FAA Report No. DOT/FAA/DS-89/19*, 552 pp.
- Turnbull, D., J. McCarthy, J. Evans, D. Zrnic', 1989: The FAA Terminal Doppler Weather Radar (TDWR) program. Preprints, *3rd International Conference on the Aviation Weather System*, Anaheim, CA, Amer. Meteor. Soc., 414-419.
- University Corporation for Atmospheric Research, 1990: Network Expansion LLWAS Algorithm Specification.